NJC

LETTER

View Article Online
View Journal | View Issue

Cite this: *New J. Chem.*, 2015, 39, 2396

Received (in Montpellier, France) 19th November 2014, Accepted 6th January 2015

DOI: 10.1039/c4nj02093f

www.rsc.org/njc

A UiO-66 analogue with uncoordinated carboxylic acids for the broad-spectrum removal of toxic chemicals†

Jared B. DeCoste,*[a] Tyler J. Demasky,[a] Michael J. Katz,[b] Omar K. Farha*[bc] and Joseph T. Hupp*[b]

Zirconium-based metal–organic frameworks (MOFs) are of great importance as sorbents due to their increased chemical and thermal stability when compared to other MOF families. Here we report a novel analogue of UiO-66 modified with oxalic acid *via* solvent-assisted ligand incorporation. This analogue has the ability to remove ammonia, cyanogen chloride, sulphur dioxide, nitrogen dioxide and octane at levels greater than or equal to the base UiO-66. We report here the highest known capacities exhibited by a MOF for SO_2 and NO_2, at pressures less than 0.10 bar and at room temperature, by UiO-66-ox. Furthermore, we show here the importance of the secondary building unit of the MOF in the removal of ammonia and cyanogen chloride.

Metal–organic frameworks (MOFs), hybrid structures composed of organic linkers connected by inorganic nodes, have been of great interest in various fields including, but not limited to, gas storage,[1–8] separations,[9–11] sensing,[12–14] and toxic gas removal.[15–17] In the area of toxic gas removal, very few materials have shown the ability to remove a broad spectrum of toxic chemicals with a single component. However, various strategies have been investigated to remove a broad spectrum of chemicals in a single material, including the impregnation of amines and metal salts on carbons,[18–20] grafting of functional groups into microporous materials,[21] and the creation of composites of materials with different chemistries.[22]

UiO-66 (Fig. 1) and its analogues have been of particular interest for the adsorption of toxic gases under ambient conditions due to their high chemical stability and ease of tailoring through the incorporation of pendant groups.[23–26] The chemical stability of these MOFs is due to the strong bonding between Zr(IV) and carboxylate oxygen atoms.[23,27] Herein, we report on the synthesis of a UiO-66 analogue featuring free carboxylic acid groups (UiO-66-ox). The acids are present as the distal carboxylates of half-protonated, non-structural ligands – specifically oxalic acid – *via* solvent-assisted ligand incorporation (SALI). Importantly, UiO-66-ox has the ability to remove ammonia, sulphur dioxide, nitrogen dioxide and octane from gas streams with efficiency greater than that of UiO-66, while maintaining the high capacity of UiO-66 for cyanogen chloride.

Using a synthesis method developed by Katz *et al.*, UiO-66 was produced with missing linkers, leading to vacancies at sites where terephthalic linkers would be incorporated in a perfect UiO-66 crystal.[28] This material will be referred to as UiO-66-vac. Defect-laden UiO-66 has been of particular interest in the literature for various applications, particularly in catalysis and for post-synthetic modification.[29] The vacant sites were exploited through a reaction with oxalic acid, where one carboxylate group coordinates with the secondary building unit (SBU) and the other carboxylic acid group is free in the pore of the MOF (Scheme 1). For comparison, UiO-66 was treated with oxalic acid in the same fashion as UiO-66-vac; however, no reaction was observed.

X-ray diffraction data (Fig. S1, ESI†) indicate that UiO-66-ox exhibits the same crystal structure as UiO-66. However, the BET surface areas of the three materials show some variance as determined from their N_2 isotherms (Fig. S2, ESI†). UiO-66, UiO-66-vac, and UiO-66-ox have BET surface areas of 990, 1590, and 1410 $m^2\ g^{-1}$, respectively. This variation in their surface areas is expected, as the increase in the surface area of UiO-66-vac when compared to that of UiO-66 is due to the missing linkers that in turn decrease the overall mass while exposing new surfaces within the small triangular windows.[28,30] It was previously shown that the surface area of UiO-66-vac is in good agreement with four of the twelve linkers missing per SBU.[28] The subsequent decrease in the BET surface area of UiO-66-ox when compared to that of UiO-66-vac is anticipated and is consistent with the increase in

[a] *Leidos, Inc., PO Box 68, Gunpowder, MD 21010, USA. E-mail: jared.b.decoste2.ctr@mail.mil*
[b] *Department of Chemistry and the International Institute for Nanotechnology, Northwestern University, 2145 Sheridan Road, Evanston, IL 60108-2112, USA. E-mail: o-farha@northwestern.edu, j-hupp@northwestern.edu*
[c] *Department of Chemistry, Faculty of Science, King Abdulaziz University, Jeddah, Saudi Arabia*

† Electronic supplementary information (ESI) available: Experimental procedures, X-ray diffraction spectra, N_2 isotherms, Fourier-transform infrared spectra, and breakthrough curves. See DOI: 10.1039/c4nj02093f

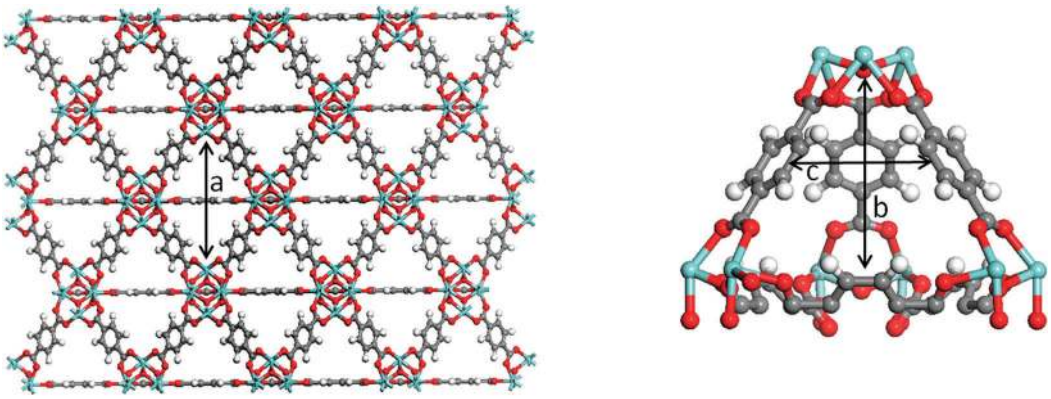

Fig. 1 (left) Depiction of UiO-66 viewed along an axis where its large octahedral cages with a diameter of ~1.6 nm (a) are visible. (right) Depiction of one tetrahedral cage of UiO-66 with a bisection of window diameters of ~1.0 nm (b) and ~0.6 nm between each benzene ring (c).

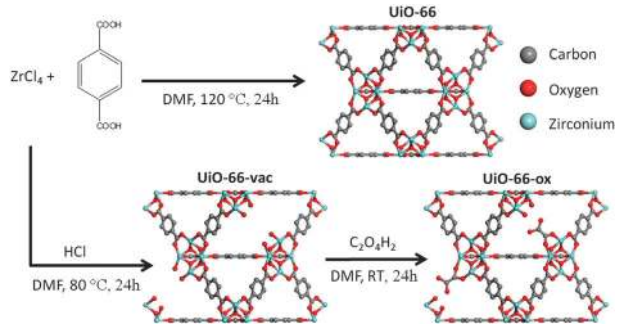

Scheme 1 Synthesis of UiO-66, UiO-66-vac, and UiO-66-ox.

the mass due to the oxalic acid group without a substantial increase in the absolute surface area. Through ^{13}C NMR of an H_2SO_4-digested UiO-66-ox sample, it was confirmed that the oxalic acid to terephthalic acid ratio was approximately 0.3, which is in good agreement with approximately half of the vacated linker sites being occupied. This is to be expected as each vacated terephthalic acid linker creates two vacancy sites that are across from one another, and only one of these sites can be modified with an oxalic acid molecule due to sterics. Upon examination of the attenuated total reflectance Fourier-transform infrared (ATR-FTIR) spectra (Fig. S3, ESI†), the characteristic carboxylic acid band in UiO-66-ox is observed at $\nu \sim 1690\ cm^{-1}$. Furthermore, a new band appears at $\nu \sim 745\ cm^{-1}$, which is the region where Zr–O bonding occurs, corresponding to a new mode due to the formation of Zr–carboxylate bonds upon the coordination of oxalic acid.[31]

A summary of microbreakthrough results (Fig. S4–S8, ESI†) can be found in Table 1. UiO-66-vac does not exhibit an increase in capacity when compared to UiO-66 for the toxic gases studied here, except for octane, despite the increased surface area and total N_2 adsorption. The lack of an increase in the adsorption of the adsorbates studied, despite the substantial increase in the space for adsorbates to fit in the MOF pores, is due to the decrease in sites that the adsorbates can interact with, within the framework. However, the substantial increase in octane adsorption by UiO-66-vac, is due to octane being a larger adsorbate whose adsorption relies purely on the physisorption phenomenon, and therefore resulting in an enhancement in its adsorption capacity due to the increased freedom of motion within the pores. Conversely, UiO-66-ox shows a significant increase in capacity over UiO-66 for SO_2 and NO_2, with a moderate increase for NH_3, while the capacity for ClCN remains relatively unchanged. The amount of octane adsorbed by UiO-66-ox was greater than that adsorbed by UiO-66, but less than that adsorbed by UiO-66-vac, which fits the trend observed for the surface area from N_2 adsorption.

Table 1 Measured microbreakthrough capacities (mmol g^{-1}) of each MOF for ammonia, cyanogen chloride, sulphur dioxide, nitrogen dioxide, and octane. Calculations per SBU and volume can be found in Tables S2 and S3 (ESI)

	NH_3	ClCN	SO_2	NO_2	C_8H_{18}
UiO-66	2.0	1.7	0.1	3.8	2.3
UiO-66-vac	1.6	0.8	0.0	3.9	4.0
UiO-66-ox	2.5	1.6	0.8	8.4	2.8

The adsorption of NH_3 by UiO-66 is likely dominated by hydrogen bonding to the SBU, and subsequently to other NH_3 molecules, as there is no change in the MOF due to covalent bonding with NH_3, as evident in the FTIR spectrum (Fig. S9, ESI†).[32] The increase in capacity for NH_3 in UiO-66-ox can be explained by two phenomena. First, NH_3 can undergo an acid–base type reaction with the free carboxylic acid groups to form an ammonium carboxylate species. This has been observed in less stable MOFs involving the degradation of the structure; however, in this case there are actually free carboxylic acid groups to react with ammonia.[33] Second, NH_3 can bind to carboxylic acid by hydrogen bonding, increasing the physisorption capacity.[34] Together these effects are a possible explanation for the increase in the ammonia capacity of UiO-66-ox over UiO-66 and UiO-66-vac. Interestingly, a decrease in NH_3 capacity for UiO-66-vac was observed when compared to UiO-66 despite the increase in the surface area and pore volume, indicating a reduction in the number of adsorption sites in UiO-66-vac.

UiO-66 and UiO-66-ox show similar capacities of 1.7 and 1.6 mmol g^{-1}, respectively, for ClCN. On the other hand, UiO-66-vac shows a considerable drop in capacity to 0.8 mmol g^{-1}, similar to the decrease observed for NH_3. We speculate that this drop in capacity might be due to the change in the SBU (see Scheme 1).

Metal oxides, including zirconia, having sites similar to the SBU, have been shown to have the ability to adsorb ClCN.[35–37] If the electronics of these M–O–M sites are perturbed in UiO-66-vac, they would not be available to aid in the chemisorption of ClCN. On the other hand, upon the reaction to form UiO-66-ox, the vacant sites are again coordinated to a carboxylate group, restoring the order to the SBU, indicating that the adsorption of ClCN depends on the electronics of the SBU being maintained.

Substantial increases in capacities are observed for SO_2 and NO_2 in UiO-66-ox when compared to the modest increase in NH_3 capacity. A capacity of 0.8 mmol g^{-1} in UiO-66-ox represents the highest reported capacity known for the room temperature adsorption of SO_2 at pressures less than 0.10 bar, for a MOF that does not contain coordinatively unsaturated metal sites.[16,38,39] The low uptake in UiO-66 indicates the lack of interaction between SO_2 and the SBU; therefore, the increase in capacity in the case of UiO-66-ox is due to a chemisorption interaction between the free carboxylic acid group and SO_2. This capacity is consistent with $\sim$1.0 SO_2 molecule per SBU or free carboxylic acid. After microbreakthrough testing was performed, dry nitrogen was run through the sample, allowing any loosely bound SO_2 to desorb, and therefore leaving only the tightly bound chemisorbed species in the MOF for post-breakthrough analysis. The ATR-FTIR spectrum for UiO-66-ox exposed to SO_2 (Fig. 2) shows S–O stretches at approximately 1076, 1049, 999, and 988 cm^{-1}. It does not seem likely that these bands would be indicative of a species interacting with the SBU, as these could be observed in UiO-66 as well. The bands are characteristic of the S=O species bound to the MOF, leading us to hypothesize on the formation of a C(=O)OSO_2 species that is tightly bound to the MOF through the free carboxylate group on UiO-66-ox.[40]

The highest observed capacity for any adsorbate studied here was for NO_2 in the case of UiO-66-ox. The addition of oxalic acid led to more than doubling of the NO_2 capacity to 8.4 mmol g^{-1}, compared to 3.8 and 3.9 mmol g^{-1} for UiO-66 and UiO-66-vac, respectively. This increase is consistent with $\sim$6.3 NO_2 molecules per SBU or free carboxylic acid. This is beyond adsorption that can be explained by a stoichiometric reaction. There are not many reports on NO_2 capacity in MOFs; albeit, this is the highest known reported value in the literature for a dynamic breakthrough test.[16,41,42] Unlike the adsorption of NH_3 and ClCN, it does not appear that the interaction with the SBU requires the SBU to be fully intact, as observed for NH_3 and CNCl, as the capacities of UiO-66 and UiO-66-vac are comparable. In fact, it was hypothesized by Ebrahim *et al.* that the adsorption of NO_2 by UiO MOFs is driven by two processes.[41] First, NO_2 molecules bind to the Zr–O sites of the SBU; second, NO_2 breaks the carboxylate coordination with the SBU, leading to the nitrate species on the SBU, and subsequent NO_2 molecules can react with the cleaved ligand. This hypothesis is strengthened by our finding that the presence of free carboxylic acid increases the NO_2 capacity, and that the XRD pattern of UiO-66-ox exposed to NO_2 shows structural degradation (Fig. S10, ESI†). The chemisorption of NO_2 by UiO-66-ox shows the appearance of new infrared bands, as seen in Fig. 1. The band at 1700 cm^{-1} is indicative of perturbation to the carboxylate groups, while the band at 1245 cm^{-1}, which does not appear in the adsorption of NO_2 by UiO-66 or UiO-66-vac, is consistent with oxidation of NO_2 by carboxylic acid to form a nitrate species. By looking more closely at the shape of the breakthrough curves (Fig. S7, ESI†), it can be seen that while the breakthrough of NO_2 against UiO-66 happens almost immediately, with only about 20% of NO_2 being removed for a long period of time, approximately 95% of the NO_2 is being removed from the toxic gas stream by UiO-66-vac for an extended period of time. These two extremely different wave front behaviours, with similar final capacities, are indicative of a slower reaction due to inaccessibility of sites on UiO-66, while the sites on UiO-66-vac are more accessible. This is consistent with the reaction taking place on the SBU, where UiO-66-vac is initially less sterically hindered than UiO-66, but as the reaction proceeds more sites are free to react with incoming NO_2.

In conclusion, the incorporation of the free carboxylic acid functional groups into UiO-66 allows for the removal of a broad spectrum of toxic chemicals not only through physical interactions, but through chemisorption as well. The increased capacity for NH_3 is due to an acid–base interaction with the carboxylic acid groups, while the increased capacities for SO_2 and NO_2 are due to the reactive capabilities of carboxylic acids. Furthermore, the incorporation of the carboxylic acid groups through a reaction with oxalic acid does not decrease the CNCl capacity of the MOF, indicating that the sites on the SBU responsible for this chemisorption, along with the removal of NH_3, remain intact. The novel synthesis of UiO-66-ox shown here can be used to create free carboxylic acid groups in other MOFs with vacancies, for various applications.

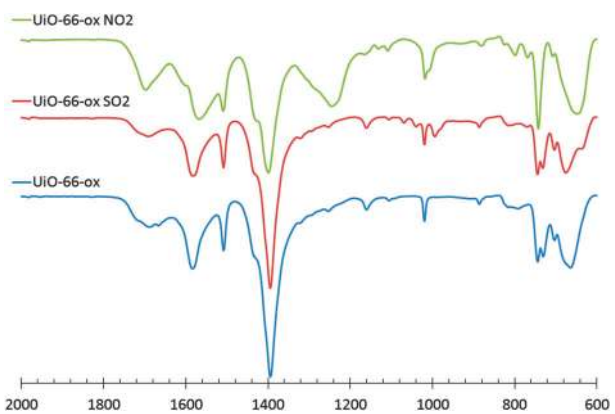

Fig. 2 ATR-FTIR spectra of UiO-66-ox exposed to SO_2 and NO_2, from 2000 to 600 cm^{-1}; compared to the UiO-66-ox spectrum.

Experimental

UiO-66-ox was synthesized by reacting an oxalic acid solution with UiO-66-vac, which was synthesized by reacting $ZrCl_4$ and terephthalic acid in a solution of DMF with HCl. Samples were activated *via* Soxhlet extraction with methanol and subsequent heating to 150 °C under vacuum. Microbreakthrough experiments were conducted on 10–15 mg of the material at 20 °C

(dew point −40 °C) and a flow rate of 20 mL min^{-1}, with the effluent monitored by gas chromatography using an appropriate detector for each gas.

Acknowledgements

J.B.D gratefully acknowledges the Defense Threat Reduction Agency (DTRA) for financial support under BA13PHM210. O.K.F and J.T.H. gratefully acknowledge the funding from the Army Research Office (project number W911NF-13-1-0229). The authors would also like to thank Stephanie Marzen for assistance with NMR experiments and David Tevault for technical editing.

Notes and references

1 S. S. Han, J. L. Mendoza-Cortes and W. A. Goddard Iii, *Chem. Soc. Rev.*, 2009, **38**, 1460–1476.
2 K. Sumida, D. L. Rogow, J. A. Mason, T. M. McDonald, E. D. Bloch, Z. R. Herm, T.-H. Bae and J. R. Long, *Chem. Rev.*, 2011, **112**, 724–781.
3 M. P. Suh, H. J. Park, T. K. Prasad and D.-W. Lim, *Chem. Rev.*, 2011, **112**, 782–835.
4 R. B. Getman, Y.-S. Bae, C. E. Wilmer and R. Q. Snurr, *Chem. Rev.*, 2011, **112**, 703–723.
5 H. Wu, Q. Gong, D. H. Olson and J. Li, *Chem. Rev.*, 2012, **112**, 836–868.
6 T. Duren, Y.-S. Bae and R. Q. Snurr, *Chem. Soc. Rev.*, 2009, **38**, 1237–1247.
7 J. Liu, P. K. Thallapally, B. P. McGrail, D. R. Brown and J. Liu, *Chem. Soc. Rev.*, 2012, **41**, 2308–2322.
8 J. B. DeCoste, M. H. Weston, P. E. Fuller, T. M. Tovar, G. W. Peterson, M. D. LeVan and O. K. Farha, *Angew. Chem., Int. Ed.*, 2014, **53**, 14092–14095.
9 J.-R. Li, R. J. Kuppler and H.-C. Zhou, *Chem. Soc. Rev.*, 2009, **38**, 1477–1504.
10 J.-R. Li, J. Sculley and H.-C. Zhou, *Chem. Rev.*, 2011, **112**, 869–932.
11 Q. Yang, D. Liu, C. Zhong and J. R. Li, *Chem. Rev.*, 2013, **113**, 8261–8323.
12 L. E. Kreno, K. Leong, O. K. Farha, M. Allendorf, R. P. Van Duyne and J. T. Hupp, *Chem. Rev.*, 2011, **112**, 1105–1125.
13 Y. Cui, Y. Yue, G. Qian and B. Chen, *Chem. Rev.*, 2011, **112**, 1126–1162.
14 J. Rocha, L. D. Carlos, F. A. A. Paz and D. Ananias, *Chem. Soc. Rev.*, 2011, **40**, 926–940.
15 N. A. Khan, Z. Hasan and S. H. Jhung, *J. Hazard. Mater.*, 2013, **244–245**, 444–456.
16 J. B. DeCoste and G. W. Peterson, *Chem. Rev.*, 2014, **114**, 5695–5727.
17 E. Barea, C. Montoro and J. A. Navarro, *Chem. Soc. Rev.*, 2014, **43**, 5419–5430.
18 J. W. H. Smith, P. Westreich, H. Abdellatif, P. Filbee-Dexter, A. J. Smith, T. E. Wood, L. M. Croll, J. H. Reynolds and J. R. Dahn, *J. Hazard. Mater.*, 2010, **180**, 419–428.
19 J. W. H. Smith, P. Westreich, A. J. Smith, H. Fortier, L. M. Croll, J. H. Reynolds and J. R. Dahn, *J. Colloid Interface Sci.*, 2010, **341**, 162–170.
20 C. Petit, C. Karwacki, G. Peterson and T. J. Bandosz, *J. Phys. Chem. C*, 2007, **111**, 12705–12714.
21 A. M. B. Furtado, D. Barpaga, L. A. Mitchell, Y. Wang, J. B. DeCoste, G. W. Peterson and M. D. LeVan, *Langmuir*, 2012, **28**, 17450–17456.
22 G. W. Peterson, J. A. Rossin, J. B. DeCoste, K. L. Killops, M. Browe, E. Valdes and P. Jones, *Ind. Eng. Chem. Res.*, 2013, **52**, 5462–5469.
23 J. H. Cavka, S. Jakobsen, U. Olsbye, N. Guillou, C. Lamberti, S. Bordiga and K. P. Lillerud, *J. Am. Chem. Soc.*, 2008, **130**, 13850–13851.
24 M. Kandiah, M. H. Nilsen, S. Usseglio, S. Jakobsen, U. Olsbye, M. Tilset, C. Larabi, E. A. Quadrelli, F. Bonino and K. P. Lillerud, *Chem. Mater.*, 2010, **22**, 6632–6640.
25 J. B. DeCoste, G. W. Peterson, H. Jasuja, T. G. Glover, Y.-G. Huang and K. S. Walton, *J. Mater. Chem. A*, 2013, **1**, 5642–5650.
26 J. B. DeCoste, G. W. Peterson, B. J. Schindler, K. L. Killops, M. A. Browe and J. J. Mahle, *J. Mater. Chem. A*, 2013, **1**, 11922.
27 J. E. Mondloch, W. Bury, D. Fairen-Jimenez, S. Kwon, E. J. DeMarco, M. H. Weston, A. A. Sarjeant, S. T. Nguyen, P. C. Stair, R. Q. Snurr, O. K. Farha and J. T. Hupp, *J. Am. Chem. Soc.*, 2013, **135**, 10294–10297.
28 M. J. Katz, Z. J. Brown, Y. J. Colon, P. W. Siu, K. A. Scheidt, R. Q. Snurr, J. T. Hupp and O. K. Farha, *Chem. Commun.*, 2013, **49**, 9449–9451.
29 G. C. Shearer, S. Chavan, J. Ethiraj, J. G. Vitillo, S. Svelle, U. Olsbye, C. Lamberti, S. Bordiga and K. P. Lillerud, *Chem. Mater.*, 2014, **26**, 4068–4071.
30 L. Sarkisov and A. Harrison, *Mol. Simul.*, 2011, **37**, 1248–1257.
31 L. Valenzano, B. Civalleri, S. Chavan, S. Bordiga, M. H. Nilsen, S. Jakobsen, K. P. Lillerud and C. Lamberti, *Chem. Mater.*, 2011, **23**, 1700–1718.
32 H. Jasuja, G. W. Peterson, J. B. Decoste, M. A. Browe and K. S. Walton, *Chem. Eng. Sci.*, DOI: 10.1016/j.ces.2014.08.050.
33 G. W. Peterson, G. W. Wagner, A. Balboa, J. Mahle, T. Sewell and C. J. Karwacki, *J. Phys. Chem. C*, 2009, **113**, 13906–13917.
34 K. C. Kim, D. Yu and R. Q. Snurr, *Langmuir*, 2013, **29**, 1446–1456.
35 S. Kim, D. C. Sorescu and J. T. Yates, *J. Phys. Chem. C*, 2007, **111**, 18226–18235.
36 T. G. Glover, J. B. DeCoste, D. Sabo and Z. J. Zhang, *Langmuir*, 2013, **29**, 5500–5507.
37 G. W. Peterson, G. W. Wagner, J. H. Keller and J. A. Rossin, *Ind. Eng. Chem. Res.*, 2010, **49**, 11182–11187.
38 D. Britt, D. Tranchemontagne and O. M. Yaghi, *Proc. Natl. Acad. Sci. U. S. A.*, 2008, **105**, 11623–11627.
39 T. G. Glover, G. W. Peterson, B. J. Schindler, D. Britt and O. Yaghi, *Chem. Eng. Sci.*, 2011, **66**, 163–170.
40 H. A. Al-Hosney and V. H. Grassian, *Phys. Chem. Chem. Phys.*, 2005, **7**, 1266–1276.
41 A. M. Ebrahim, B. Levasseur and T. J. Bandosz, *Langmuir*, 2012, **29**, 168–174.
42 B. Levasseur, C. Petit and T. J. Bandosz, *ACS Appl. Mater. Interfaces*, 2010, **2**, 3606–3613.